Electronic Supplementary Material (ESI) for Energy & Environmental Science.

Supporting Information (SI)

Highly selective gas separation membrane using in-situ amorphised metal-organic frameworks

Aylin Kertik,[a] Lik H. Wee*[a], Martin Pfannmöller,[b] Sara Bals,[b] Johan A. Martens[a] and Ivo F.J. Vankelecom*[a]

[a]*Centre for Surface Chemistry and Catalysis, University of Leuven, Celestijnenlaan 200f, B3001, Heverlee, Leuven, Belgium. E-mail: likhong.wee@kuleuven.be; ivo.vankelecom@kuleuven.be*

[b]*Electron Microscopy for Materials Science, University of Antwerp, Groenenborgerlaan 171, B2020, Antwerp, Belgium.*

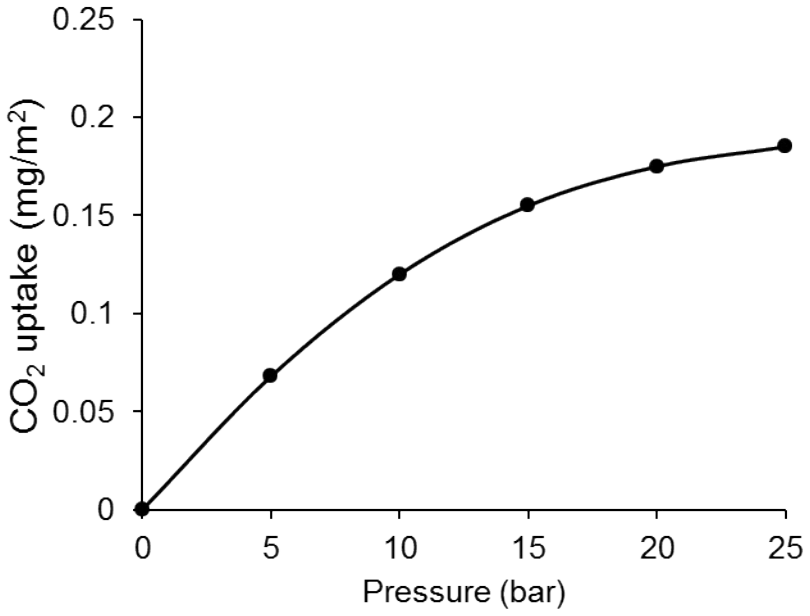

Fig. S1 CO_2 adsorption isotherm of ZIF-8 at 35 °C. Experimental data is taken from Ref. [1].

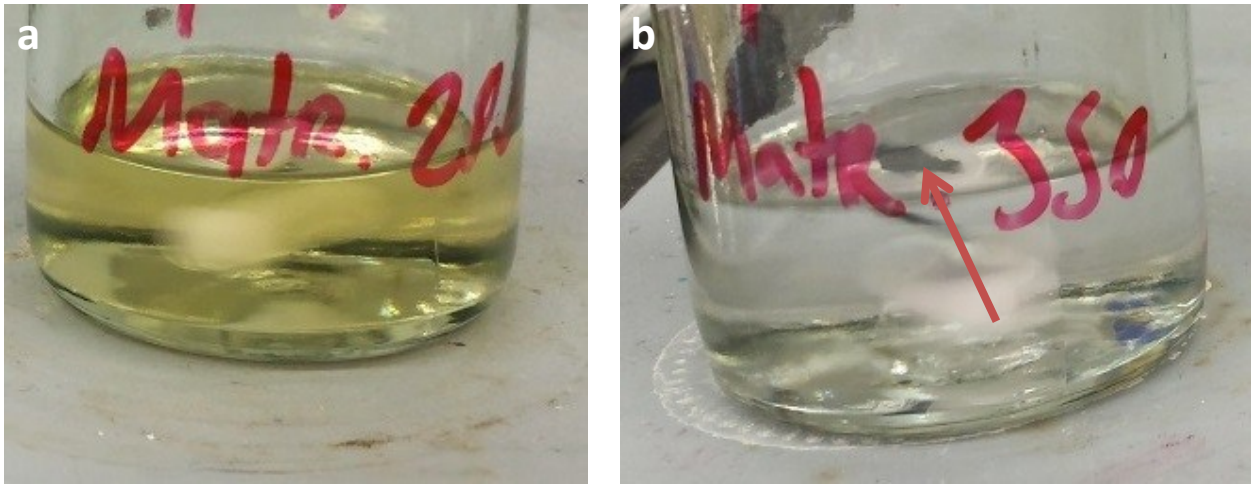

Fig. S2 The solubility of pure Matrimid® membranes after annealing at (a) 250 °C and (b) 350 °C. The latter is indicated by the red arrow.

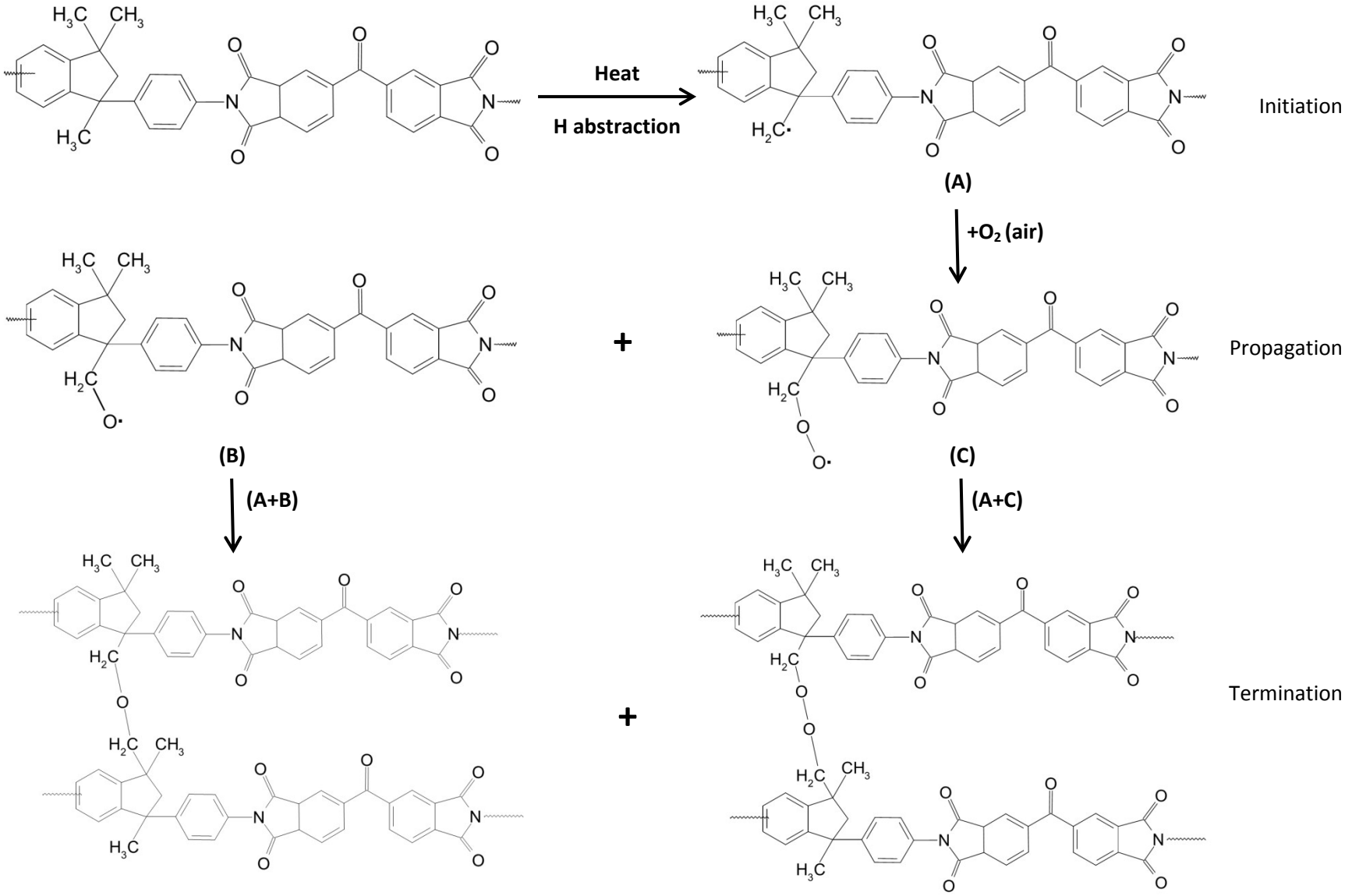

Fig. S3 The proposed thermo-oxidative cross-linking mechanism for Matrimid®.

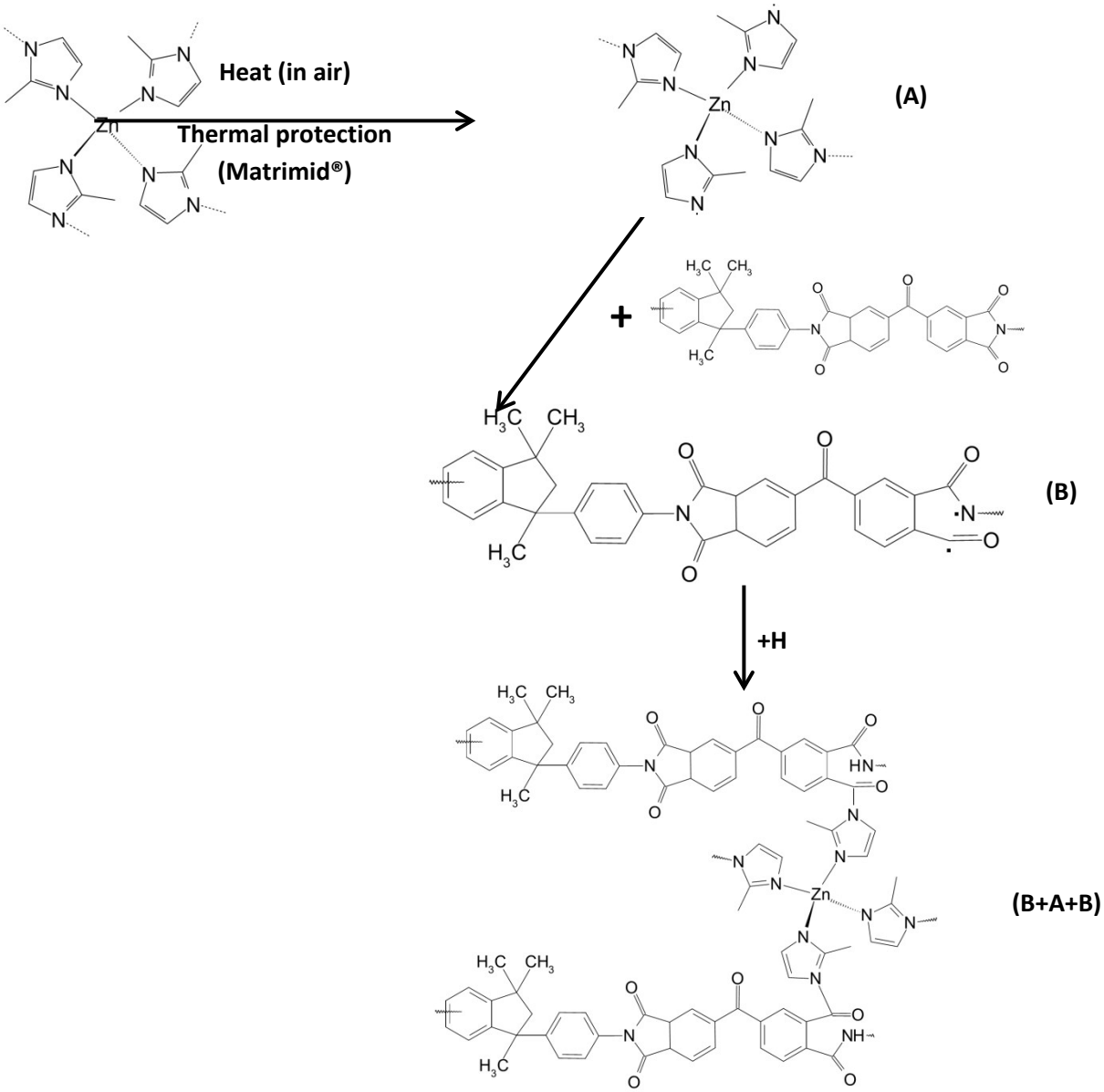

Fig. S4 The proposed cross-linking mechanism of the MOF in the MMM. It should be noted that this mechanism is shown separately for clarity. In the MMMs, this mechanism and the polymer cross-linking occur simultaneously.

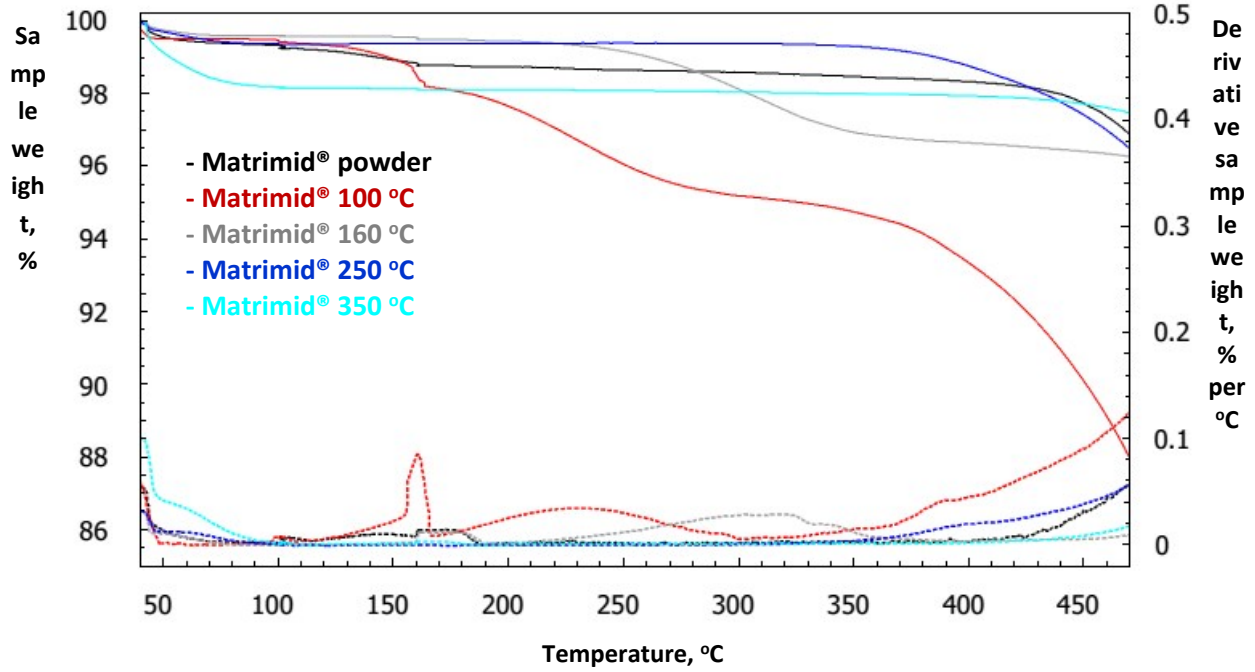

Fig. S5 The TGA plot (solid lines) and derivatives (dotted lines) of the Matrimid® membranes.

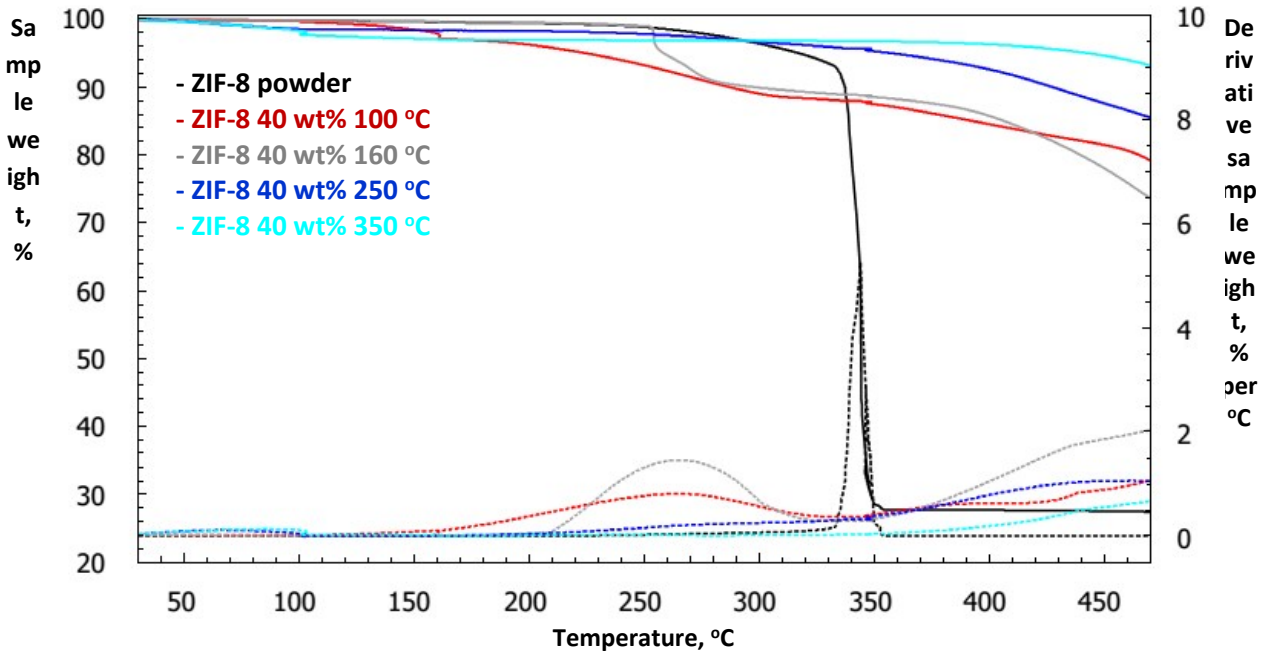

Fig. S6 The TGA plot (solid lines) and derivatives (dotted lines) for MMMs with 40 wt.% ZIF-8 loading.

Table S1 The tensile strength of Matrimid® and MMMs with 40% ZIF-8.

Sample	*Tensile strength (MPa)*
Matrimid® treated at 100 °C (M100)	85.3
Matrimid® treated at 160 °C (M160)	101.8
Matrimid® treated at 250 °C (M250)	118.6
Matrimid® treated at 350 °C (M350)	135.2
MMM with 40% ZIF-8, treated at 100 °C (Z8-40-100)	6.3
MMM with 40% ZIF-8, treated at 160 °C (Z8-40-160)	5.2
MMM with 40% ZIF-8, treated at 250 °C (Z8-40-250)	12.0
MMM with 40% ZIF-8, treated at 350 °C (Z8-40-350)	33.8

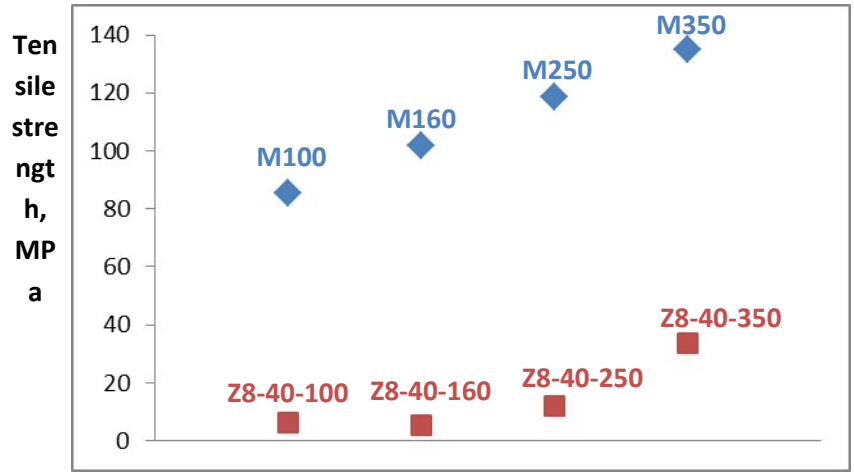

Fig. S7 The dependency of the membrane tensile strength on the heat treatment temperature.

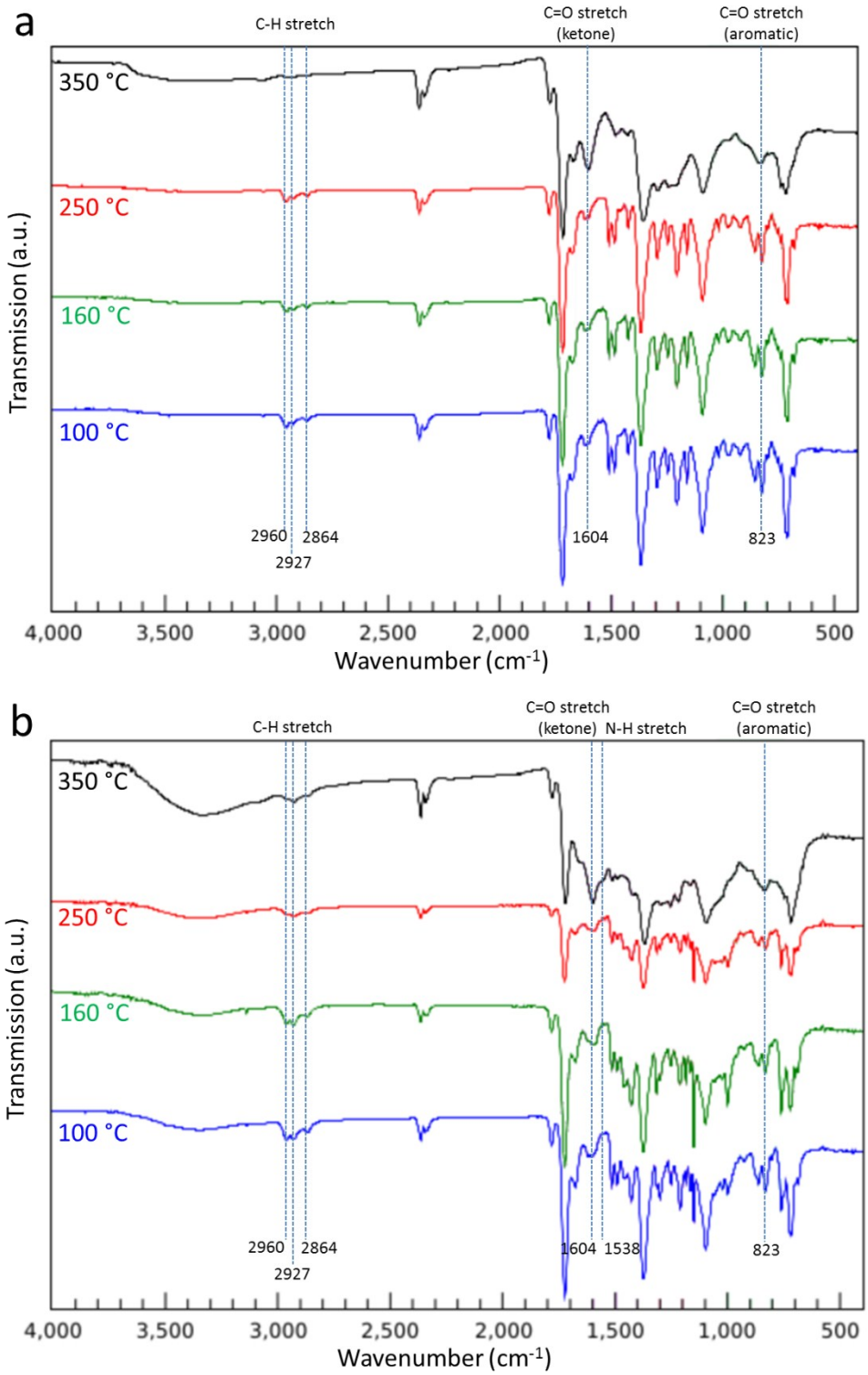

Fig. S8 The ATR-FTIR patterns of the (a) Matrimid® and (b) MMMs with 40 wt.% ZIF-8 loading as a function of temperature.

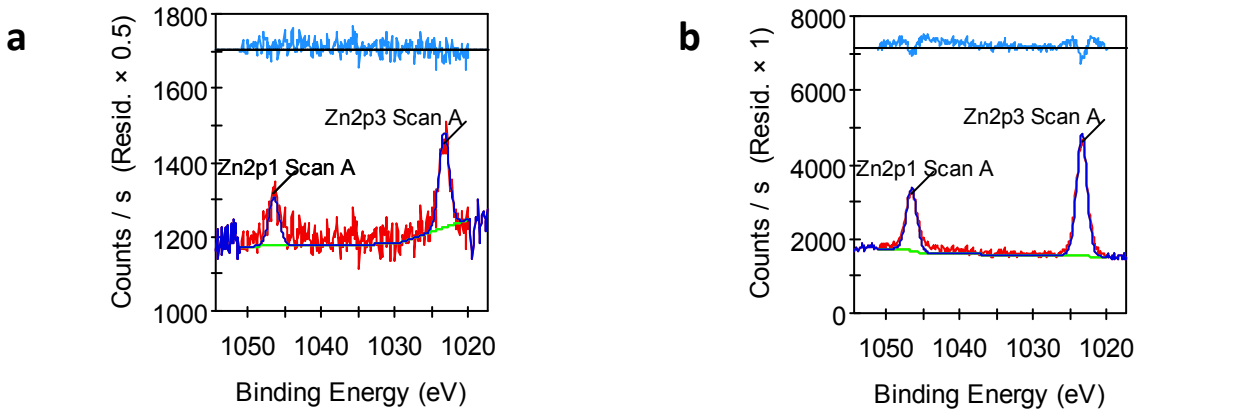

Name	*Peak BE*	*FWHM eV*	*Area (P) CPS.eV*	*Atomic %*	*Q*
Zn2p3 Scan A	1023.33	1.64	452.88	100.00	1

Name	*Peak BE*	*FWHM eV*	*Area (P) CPS.eV*	*Atomic %*	*Q*
Zn2p3 Scan A	1023.41	1.64	5799.01	100.00	1

Fig. S9 The XPS patterns of MMMs with ZIF-8 (40 wt.%) treated at (a) 100 ˚C and (b) 350 ˚C

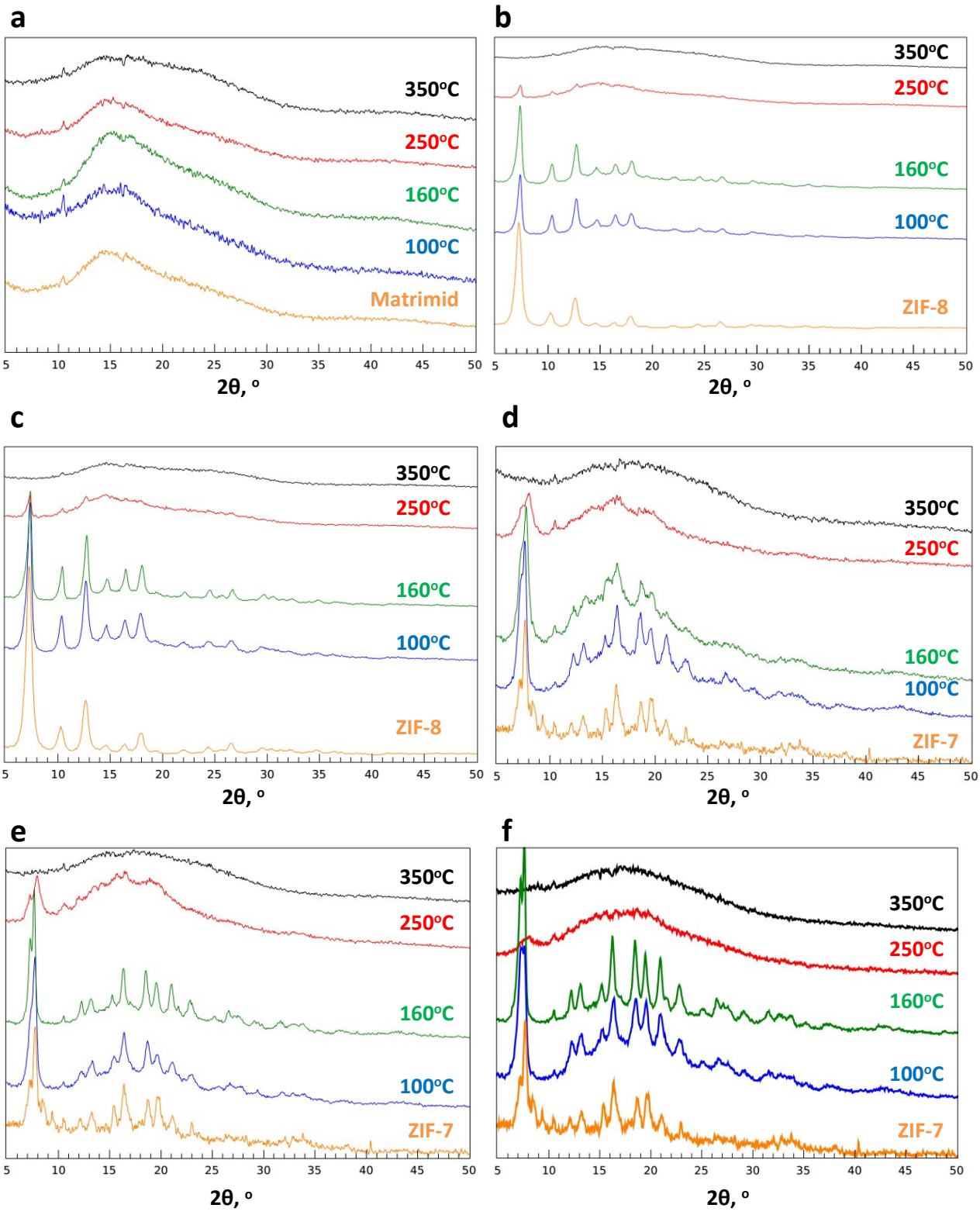

Fig. S10 The XRD plots of (a) Matrimid® and MMMs with (b) 20 wt.% and (c) 30 wt.% ZIF-8. MMMs with (d) 20 wt.%, (e) 30 wt.%, (f) 40 wt.% ZIF-7 loading are also given.

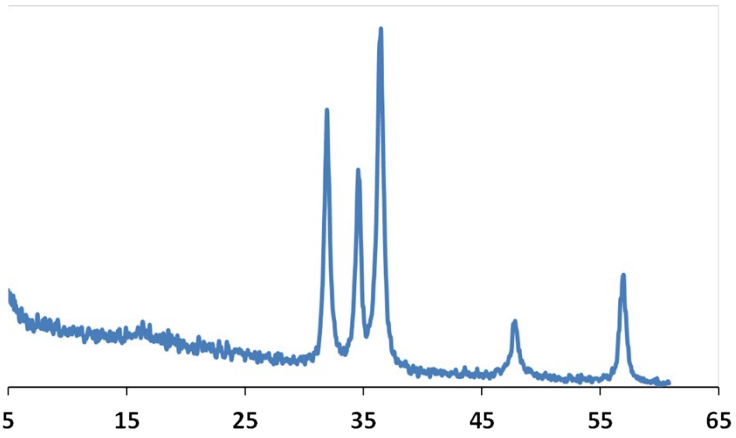

Fig. S11 The XRD pattern of ZIF-8 powder subjected to thermal treatment at 350 ˚C.

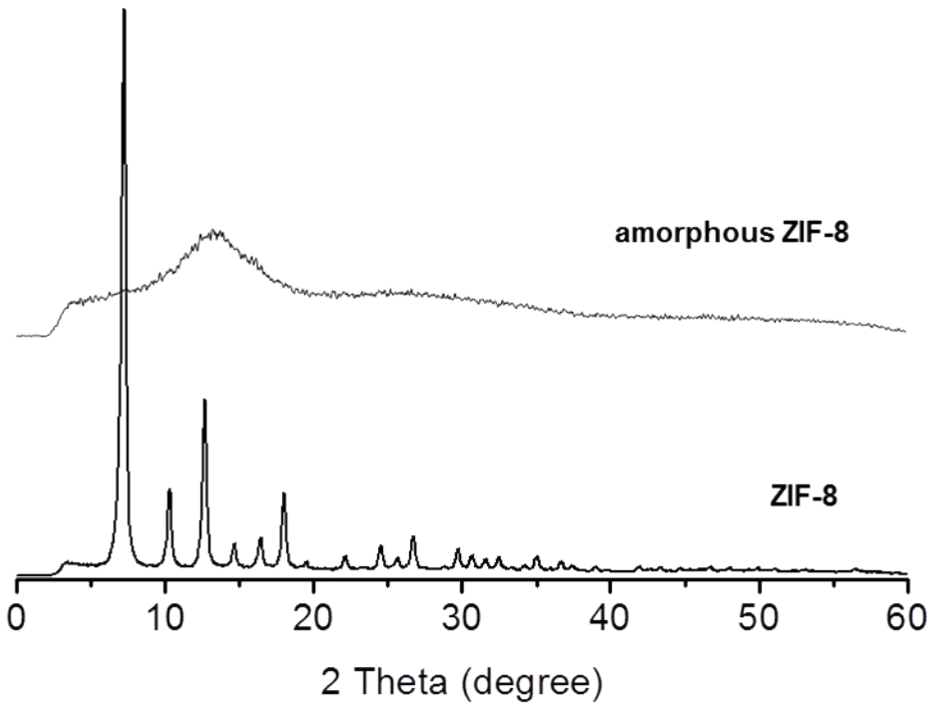

Fig. S12 XRD patterns of amorphous ZIF-8 obtained by ball-milling and as-synthesized ZIF-8.

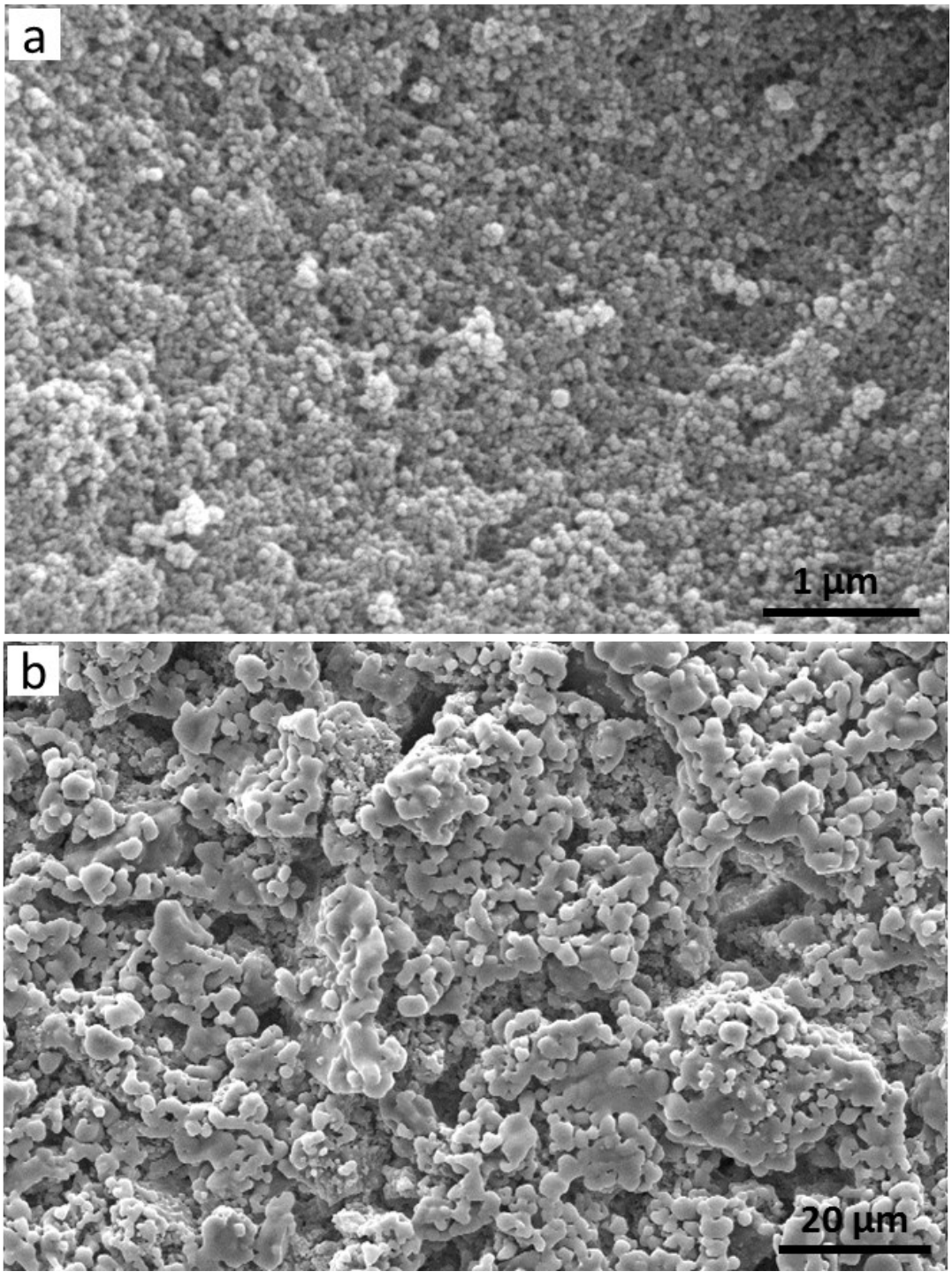

Fig. S13 SEM images of (a) as-synthesized ZIF-8 and (b) amorphous ZIF-8 obtained by ball-milling.

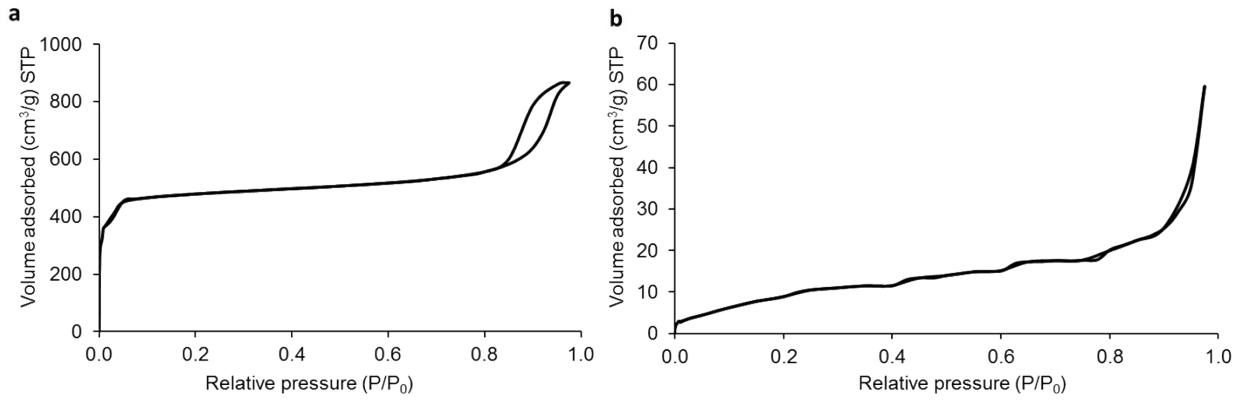

Fig. S14 N_2 adsorption-desorption isotherms of (a) as-synthesized ZIF-8 and (b) amorphous ZIF-8 prepared by ball-milling.

Table S2 Physicochemical properties of as-synthesized ZIF-8 and amorphous ZIF-8 prepared by ball-milling.

Samples	BET surface area (cm^2/g)	Micropore volume obtained from *t*-plot (cm^2/g)	Total pore volume (cm^3/g)
ZIF-8	1877	0.66	1.33
Amorphous ZIF-8	16	-	0.09

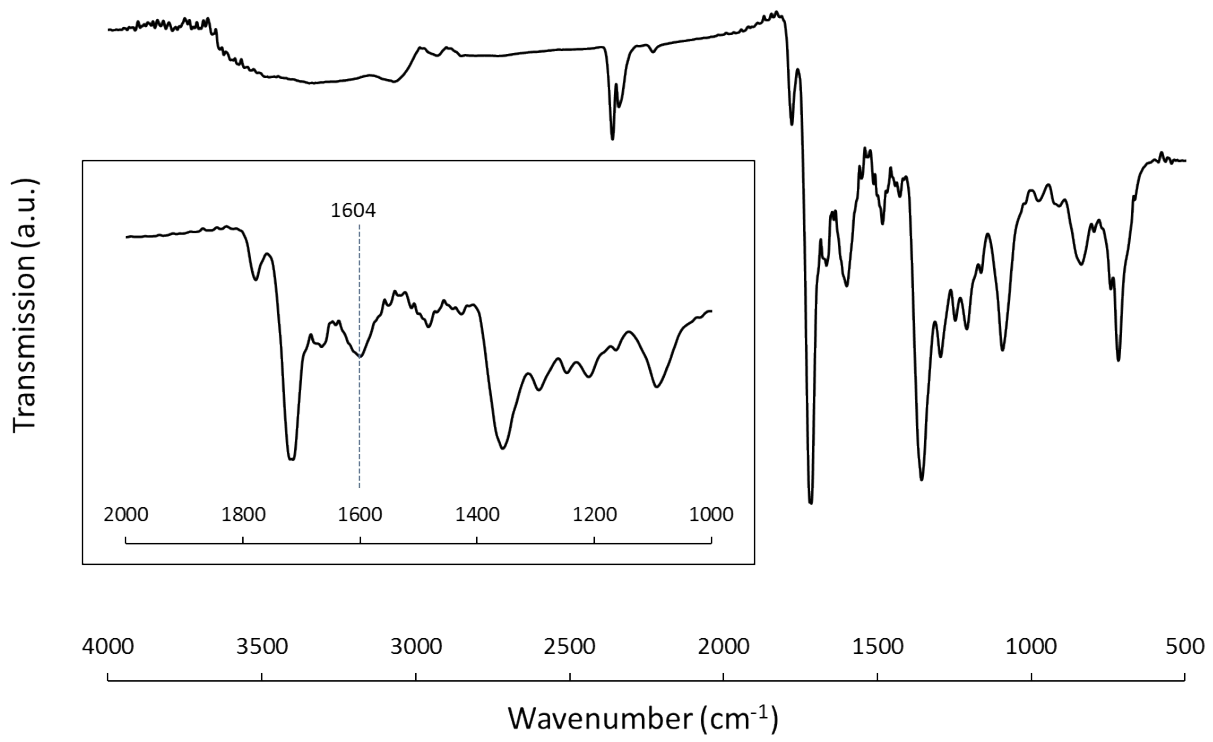

Fig. S15 ATR-FTIR spectrum of MMM prepared from amorphous ZIF-8 prepared via ball-milling. The inset shows the enlarged region from range 2000-1000 cm^{-1} indicating the peak at 1600 cm^{-1} is assigned to C=O stretching vibration attributed from polymer-polymer crosslinking.

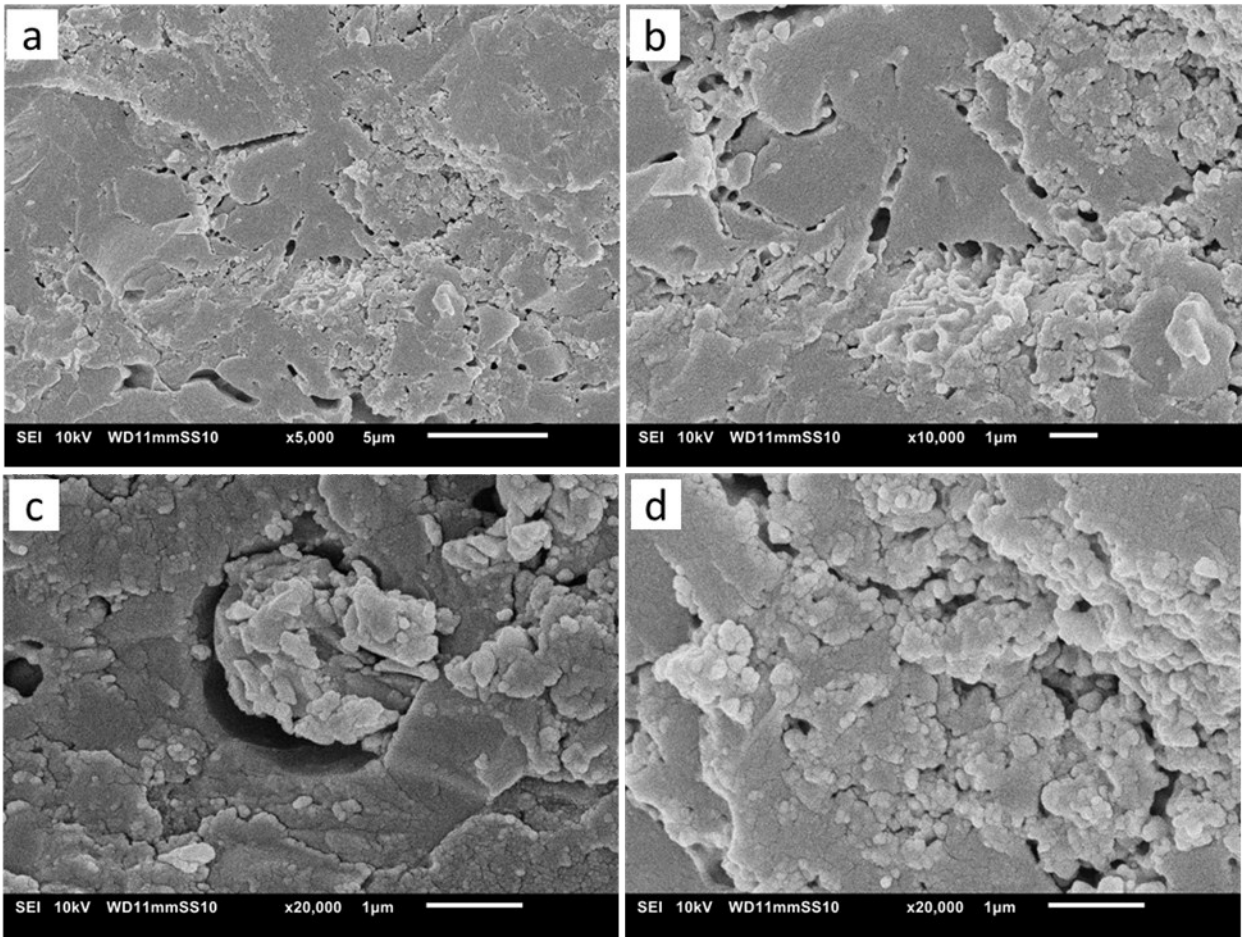

Fig. S16 (a,b) Top view and (c,d) cross-sectional SEM images of MMM filled with amorphous ZIF-8 prepared by ball-milling (30 wt.%) viewed at different magnifications.

160 °C
t= 0 days

t= 2 days

250 °C
t= 0 days

t= 2 days

350 °C
t = 2 days

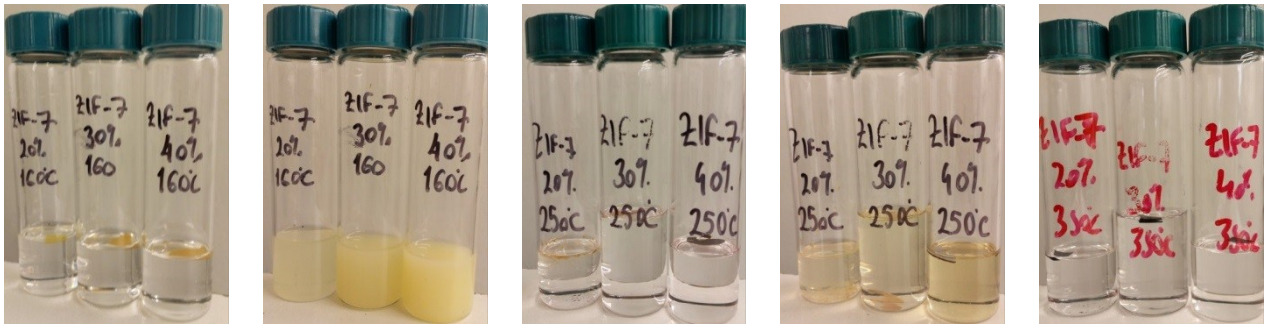

Fig. S17 The solubility of MMMs with ZIF-7, after annealing at 160 ˚C, 250 ˚C, and 350 ˚C. Similar to ZIF-8, the MMMs with ZIF-7 were effectively cross-linked by the treatment at 250 ˚C and 350 ˚C and the presence of the MOF.

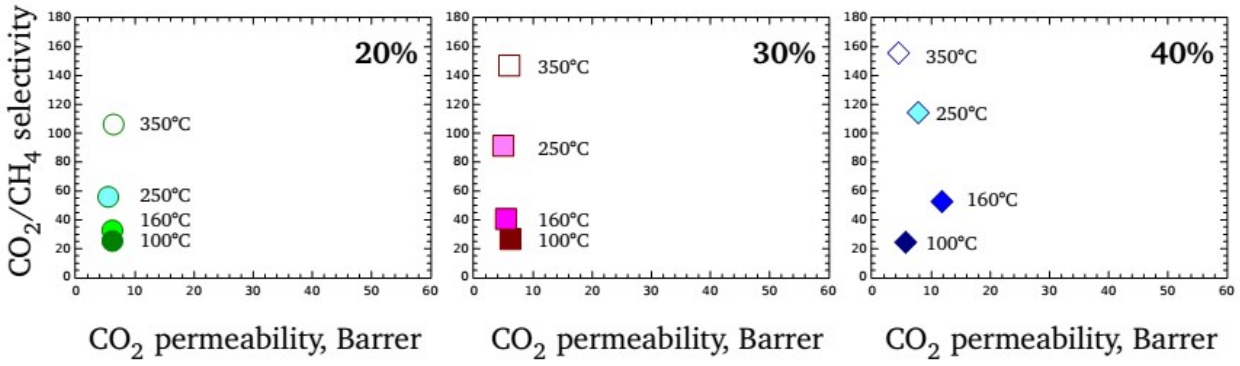

Fig. S18 The gas separation performance of the MMMs with ZIF-7.

Table S3 The gas separation data of MMMs[1] and polymeric membranes from this work and literature.

Polymer	MOF	Loading, wt.%	Treatment	Measurement conditions[2]	CO_2 permeability, Barrer[3]	CO_2/CH_4 selectivity	Ref.
Matrimid®	none	0	100 ℃, 24 h, in air	10 bar, 35 ℃, 50 vol% CO_2/50 vol% CH_4	5.6±0.7	22.3±0.2	This work
			160 ℃, 24 h, in air		8.2±0.2	31.6±1	This work
			250 ℃, 24 h, in air		5.3±0.2	40.4± 3.5	This work
			350 ℃, 24 h, in air		7.4±0.7	76.3±0.8	This work
				40 bar, 35 ℃, 50 vol% CO_2/50 vol% CH_4	2.6±0.02	90.8±4.2	This work
Matrimid®	Amorphous ZIF-8 (ball-milling)	30	350 ℃, 24 h, in air	10 bar, 35 ℃, 50 vol% CO2/50 vol% CH4	47.9±0.48	0.83±0.001	This work
Matrimid®	ZIF-8	20	100 ℃, 24 h, in air	10 bar, 35 ℃, 50 vol% CO_2/50 vol% CH_4	19.3±3.6	22.4±3.2	This work
			160 ℃, 24 h, in air		20.8±6	44.3±4.5	This work
			250 ℃, 24 h, in air		4.5±0.5	60.0±3.4	This work
			350 ℃, 24 h, in air		2.8±0.1	91.3±11.7	This work
		30	100 ℃, 24 h, in air	10 bar, 35 ℃, 50 vol% CO_2/50 vol% CH_4	19.6±4.9	18.6±4	This work
			160 ℃, 24 h, in air		46.2±9.6	24.3±2	This work
			250 ℃, 24 h, in air		3.4±0.2	111.4±18.1	This work
			350 ℃, 24 h, in air		4.5±0.6	162.0±6.6	This work
		40	100 ℃, 24 h, in air	10 bar, 35 ℃, 50 vol% CO_2/50 vol% CH_4	6.5±0.4	18.4±2.4	This work
			160 ℃, 24 h, in air		56.6±4.7	20.0±1.8	This work
			250 ℃, 24 h, in air		11.8±1.3	52.6±1.9	This work
			350 ℃, 24 h, in air		4.9±1.2	91.5±12	This work
				40 bar, 35 ℃, 50 vol% CO_2/50 vol% CH_4	1.9±0.01	134±7.6	This work
Matrimid®	ZIF-7	20	100 ℃, 24 h, in air	10 bar, 35 ℃, 50 vol% CO_2/50 vol% CH_4	6.1±1.4	25.4±1.4	This work
			160 ℃, 24 h, in air		6.1±0.7	32.8±3.9	This work
			250 ℃, 24 h, in air		5.4±0.5	56.1±1	This work
			350 ℃, 24 h, in air		5.4±1.1	112.0±8.4	This work
		30	100 ℃, 24 h, in air	10 bar, 35 ℃, 50 vol% CO_2/50 vol% CH_4	6.1±0.4	26.8±3.4	This work
			160 ℃, 24 h, in air		5.4±3.5	40.6±1.4	This work
			250 ℃, 24 h, in air		5.0±1.2	91.5±12	This work
			350 ℃, 24 h, in air		5.1±0.8	147.2±11.4	This work

		40	100 ℃, 24 h, in air	10 bar, 35 ℃, 50 vol% CO_2/50 vol% CH_4	5.7±1.5	24.5±8	This work
			160 ℃, 24 h, in air		11.8±1.3	52.6±1.9	This work
			250 ℃, 24 h, in air		7.8±2	114.4±9.6	This work
			350 ℃, 24 h, in air		4.5±1.7	155.8±11.5	This work
				40 bar, 35 ℃, 50 vol% CO_2/50 vol% CH_4	1.9±0.05	140±11.5	This work
Matrimid®	ZIF-8	20	180 ℃, 18 h, *in vacuo*	4 bar, 22 ℃	12.96	41.5	2
Matrimid®	ZIF-8	50[4]	240 ℃, overnight, *in vacuo*	2 bar, 35 ℃, 10 mol% CO_2/90 mol% CH_4	[5]	89.15	3
Matrimid®	CuBDC (nanosheet)	8.2	180 ℃, 12 h, *in vacuo*	7.5 bar, 25 ℃, equimolar CO_2/CH_4	2.78	88.2	4
Matrimid®	Ni_2(dodbc)	23	120 ℃, 24 h, *in vacuo*	10 bar, 35 ℃, equimolar CO_2/CH_4	14.7	32.5	5
Matrimid®	MIL-53	15	80 ℃, 24 h, 150℃, *in vacuo*	3 bar, 35 ℃	12.43	51.8	6
Matrimid®	Cu-BTC	30	90 ℃, 24 h	4 bar, 35 ℃, 35 vol% CO_2/65 vol% CH_4	17[6]	23	7
Matrimid®	MOF-5	10	240 ℃, 24 h, *in vacuo*	2 atm, 35 ℃	11.10	51	8
Matrimid®	MIL-53(Al)-NH_2	25	180 ℃, 10 h, *in vacuo*	3 bar, 0 ℃, equimolar CO_2/CH_4	107	3.9	9
Ultem	Cu-BTC	35	*in vacuo*	3.5 bar, 35 ℃	4.1	34	10
PEI	Cubic-MOF-5	25	70 ℃, 2 d, *in vacuo*	6 bar, 25 ℃	5.39	23.43	11
PSf	MIL-53(Al)-NH_2	25	180 ℃, 10 h, *in vacuo*	3 bar, 35 ℃, equimolar CO_2/CH_4	5.5	27.5	9
PSf	MIL-68(Al)	8	120 ℃, 24 h, *in vacuo*	2 bar, 35 ℃, equimolar CO_2/CH_4	5.7	36.5	12
PMP	MIL-53(Al)-NH_2	30	50 ℃, 12 h, *in vacuo*	30 ℃	358.2	24.4	13
ODPA-TMPDA	Cu-BTC	40	200 ℃, 24 h, *in vacuo*	2 atm, 35 ℃	260.7	27.75	10
6FDA-ODA	UiO-66	25	230 ℃, 15 h, *in vacuo*	10 bar, 35 ℃	50.4	46.1	14
Pebax	ZIF-7	34	Room temperature, 24 h	3.75 bar (CO_2), 7.5 bar (CH_4), 20 ℃	41	44	15
PVC-g-POEM	ZIF-8 (hollow	30	50 ℃, 4 h, *in*	1 bar, 35 ℃	623	11.2	16

	sphere)		*vacuo*, 24 h				
Poly(vinylidene fluoride)	Cu-BTC	10	120 ℃, 24 h, *in vacuo*	5 bar, 25 ℃	2.002	41.7	17
Poly(phenylene oxide)	Cu-BTC	40	200 ℃, 24 h, *in vacuo*	30 ℃	115	34	18
Ultem	none	0	120 ℃, 24 h, *in vacuo*	3.5 bar, 35 ℃	1.48	37	19
Poly(methyl methacrylate)	none	0	>Tg	5 atm, 35 ℃	0.35	60	20
Matrimid®	none	0	130 ℃, overnight, *in vacuo*	1 atm, 35 ℃	8.7	36.3	21
Poly(ether sulfone)	none	0	Compression molding, 300℃	10 atm, 35 ℃	2.8	28	22
PEEK	none	0	Tg+5 ℃	10 atm, 35 ℃	0.963	31	23
Brominated Matrimid® 5218 PI	none	0	250 ℃, 48 h, *in vacuo*	10 atm, 35 ℃	13.3	30.2	24
Cellulose acetate	none	0	150 ℃, 48 h, *in vacuo*	10 atm, 35 ℃	3.04	38	25
Poly(vinylidene fluoride)	none	0	120 ℃, 24 h, *in vacuo*	5 bar, 25 ℃	0.915	21.27	17
Poly(vinyl chloride)	none	0	Room temperature, 2 h, *in vacuo*	1 bar, 25 ℃	0.54	22.5	26
PDMS	none	0	75 ℃, 45 min, 25℃, 3 d	4 bar, 35 ℃	3970	4	27
Polysulfone	none	0	Tg+10 ℃, 2 d, *in vacuo*	10 atm, 35 ℃	5.6	22	28
Polycarbonate	none	0	Tg+10 ℃, several days, *in vacuo*	10 atm, 35 ℃	6.8	18.9	29
Polystyrene	none	0	85 ℃, 24 h	4.4 atm, 23 ℃	14.1	18.1	30
PPO	none	0	[6]	1 atm, 35 ℃	82	12.8	31
Ethyl cellulose	none	0	25 ℃, 20 h, 60% relative humidity	2 bar, 25 ℃	67.7	11.1	32
Torlon	none	0	250 ℃, overnight, *in vacuo*	10 atm, 35 ℃	0.83	27.8	33

[1] For each reference, the best performance was listed
[2] If a gas mixture composition is not listed, the data represents pure gas measurements
[3] 1 Barrer = [10^{-10} cm^3 (STP) cm/(cm^2 s cmHg)]
[4] Loading calculated as (wt. MOF)/(wt. polymer)
[5] Not reported
[6] Rate of permeation is reported as GPU, 1 GPU = [$10^{-6}$$cm^3$(STP)/($cm^2$ s cmHg)]= [3.35 x 10^{-10} mol/(m^2 s Pa)]

References

1. Zhang, Z. *et al.* AIChE **59**, 2195–2206 (2013).

2. Song, Q. *et al.* Zeolitic imidazolate framework (ZIF-8) based polymer nanocomposite membranes for gas separation. *Energy Environ. Sci.* **5,** 8359–8369 (2012).

3. Ordoñez, M. J. C., Balkus Jr., K. J., Ferraris, J. P. & Musselman, I. H. Molecular sieving realized with ZIF-8/Matrimid® mixed-matrix membranes. *J. Membr. Sci.* **361,** 28–37 (2010).

4. Rodenas, T. *et al.* Metal-organic framework nanosheets in polymer composite materials for gas separation. *Nat. Mater.* **14,** 48–55 (2015).

5. Bachman, J. E. & Long, J. R. Plasticization-resistant Ni_2(dobdc)/polyimide composite membranes for the removal of CO_2 from natural gas. *Energy Environ. Sci.* **9,** 2031–2036 (2016).

6. Dorosti, F., Omidkhah, M. & Abedini, R. Fabrication and characterization of Matrimid/MIL-53 mixed matrix membrane for CO_2/CH_4 separation. *Chem. Eng. Res. Des.* **92,** 2439–2448 (2014).

7. Basu, S., Cano-Odena, A. & Vankelecom, I. F. J. Asymmetric membrane based on Matrimid and polysulphone blends for enhanced permeance and stability in binary gas (CO_2/CH_4) mixture separations. *Sep. Purif. Technol.* **75,** 15–21 (2010).

8. Perez, E. V., Balkus Jr., K. J., Ferraris, J. P. & Musselman, I. H. Mixed-matrix membranes containing MOF-5 for gas separations. *J. Membr. Sci.* **328,** 165–173 (2009).

9. Rodenas, T., van Dalen, M., Serra-Crespo, P., Kapteijn, F. & Gascon, J. Mixed matrix membranes based on NH_2-functionalized MIL-type MOFs: Influence of structural and operational parameters on the CO_2/CH_4 separation performance. *Microporous Mesoporous Mater.* **192,** 35–42 (2014).

10. Duan, C., Jie, X., Liu, D., Cao, Y. & Yuan, Q. Post-treatment effect on gas separation property of mixed matrix membranes containing metal organic frameworks. *J. Membr. Sci.* **466,** 92–102 (2014).

11. Arjmandi, M. & Pakizeh, M. Mixed matrix membranes incorporated with cubic-MOF-5 for improved polyetherimide gas separation membranes: Theory and experiment. *J. Ind. Eng. Chem.* **20,** 3857–3868 (2014).

12. Seoane, B., Sebastián, V., Téllez, C. & Coronas, J. Crystallization in THF: the possibility of one-pot synthesis of mixed matrix membranes containing MOF MIL-68(Al). *CrystEngComm* **68,** 1–5 (2013).

13. Abedini, R., Omidkhah, M. & Dorosti, F. Highly permeable poly(4-methyl-1-pentyne)/NH_2 -MIL-53(Al) mixed matrix membrane for CO_2/CH_4 separation. *RSC Adv.* **4,** 36522 (2014).

14. Nik, O. G., Chen, X. Y. & Kaliaguine, S. Functionalized metal organic framework-polyimide mixed matrix membranes for CO 2 / CH 4 separation. *J. Membr. Sci.* **414,** 48–61 (2012).

15. Li, T., Pan, Y., Peinemann, K.-V. & Lai, Z. Carbon dioxide selective mixed matrix composite membrane containing ZIF-7 nano-fillers. *J. Membr. Sci.* **425-426,** 235–242 (2013).

16. Hwang, S. *et al.* Hollow ZIF-8 nanoparticles improve the permeability of mixed matrix membranes for CO_2/CH_4 gas separation. *J. Membr. Sci.* **480,** 11–19 (2015).

17. Feijani, E. A., Mahdavi, H. & Tavasoli, A. Poly(vinylidene fluoride) based mixed matrix membranes comprising metal organic frameworks for gas separation applications. *Chem. Eng. Res. Des.* **96,** 87–102 (2015).

18. Ge, L., Zhou, W., Rudolph, V. & Zhu, Z. Mixed matrix membranes incorporated with size-reduced Cu-BTC

for improved gas separation. *J. Mater. Chem. A* **1,** 6350 (2013).

19. Hao, L., Li, P. & Chung, T.-S. PIM-1 as an organic filler to enhance the gas separation performance of Ultem polyetherimide. *J. Membr. Sci.* **453,** 614–623 (2014).

20. Raymond, P. C., Koros, W. J. & Paul, D. R. Comparison of mixed and pure gas permeation characteristics for CO_2 and CH_4 in copolymers and blends containing methyl methacrylate units. *J. Membr. Sci.* **77,** 49–57 (1993).

21. Guiver, M. D. *et al.* Structural characterization and gas-transport properties of brominated Matrimid polyimide. *J. Polym. Sci. Part A Polym. Chem.* **40,** 4193–4204 (2002).

22. Chiou, J. S., Maeda, Y. & Paul, D. R. Gas permeation in polyethersulfone. *J. Appl. Polym. Sci.* **33,** 1823–1828 (1987).

23. Handa, Y. P., Roovers, J. & Moulini, P. Gas transport properties of substituted PEEKs. *J. Polym. Sci. Part B Polym. Phys.* **35,** 2355–2362 (1997).

24. Xiao, Y., Dai, Y., Chung, T.-S. & and Michael D. Guiver. Effects of brominating matrimid polyimide on the physical and gas transport properties of derived carbon membranes. *Macromolecules* **38,** 10042–10049 (2005).

25. Li, J., Nagai, K., Nakagawa, T. & Wang, S. Preparation of polyethyleneglycol (PEG) and cellulose acetate (CA) blend membranes and their gas permeabilities. *J. Appl. Polym. Sci.* **58,** 1455–1463 (1995).

26. Tiemblo, P., J. Guzmán, E. Riande, C. Mijangos & and H. Reinecke. The gas transport properties of PVC functionalized with mercapto pyridine groups. *Macromolecules* **35,** 420–424 (2002).

27. Berean, K. *et al.* The effect of crosslinking temperature on the permeability of PDMS membranes: Evidence of extraordinary CO_2 and CH_4 gas permeation. *Sep. Purif. Technol.* **122,** 96–104 (2014).

28. McHattie, J. S., Koros, W. J. & Paul, D. R. Gas transport properties of polysulphones: 1. Role of symmetry of methyl group placement on bisphenol rings. *Polymer (Guildf).* **32,** 840–850 (1991).

29. Hellums, M. W., Koros, W. J., Husk, G. R. & Paul, D. R. Fluorinated polycarbonates for gas separation applications. *J. Membr. Sci.* **46,** 93–112 (1989).

30. Chen, W.-J. & Martin, C. R. Gas-transport properties of sulfonated polystyrenes. *J. Membr. Sci.* **95,** 51–61 (1994).

31. Perego, G., Roggero, A., Sisto, R. & Valentini, C. Membranes for gas separation based on silylated polyphenylene oxide. *J. Membr. Sci.* **55,** 325–331 (1991).

32. Li, X.-G., Kresse, I., Xu, Z.-K. & Springer, J. Effect of temperature and pressure on gas transport in ethyl cellulose membrane. *Polymer (Guildf).* **42,** 6801–6810 (2001).

33. Hosseini, S. S. & Chung, T. S. Carbon membranes from blends of PBI and polyimides for N_2/CH_4 and CO_2/CH_4 separation and hydrogen purification. *J. Membr. Sci.* **328,** 174–185 (2009).